(2)

AL-TR-89-055 AD:

AD-A232 393

Final Report
for the period
May 1987 to
August 1989

Quantum Chemical Studies of Candidate High Energy Density Material Compounds

January 1991

Authors:
G.F. Adams
C.F. Chabalowski

US Army Ballistic Research Laboratory
Attn: SLCBR-DD-T
Aberdeen Proving ground MD 21005-5066

F04611-87-X-0059
F04611-87-X-0067

Approved for Public Release

Distribution is unlimited. The OL-AC PL Technical Services Office has reviewed this report and it is releaseable to the National Technical Information Service, where it will be available to the general public, including foreign nationals.

Prepared for the: **OL-AC PhillipsLaboratory (AFSC)**

Air Force Systems Command
Edwards AFB CA 93523-5000

NOTICE

When U.S. Government drawings, specifications, or other data are used for any purpose other than a definitely related Government procurement operation, the fact that the Government may have formulated, furnished, or in any way supplied the said drawings, specifications, or other data, is not to be regarded by implication or otherwise, or in any way licensing the holder or any other person or corporation, or conveying any rights or permission to manufacture, use or sell any patented invention that may be related thereto.

FOREWORD

This final report was submitted by the US Army Ballistic Research Laboratory, Aberdeen Proving Ground MD 21005-5066 on completion of MIPRs F04611-87-X-0059 and F04611-88-X-0067 with the OLAC, Phillips Laboratory (AFSC) (formerly Astronautics Laboratory), Edwards AFB CA 93523-5000. OLAC PL Project Manager was Capt Pete Dolan.

This report has been reviewed and is approved for release and distribution in accordance with the distribution statement on the cover and on the DD Form 1473.

PETER J. DOLAN, Capt, USAF
Project Manager

Stephen L. Rodgers

STEPHEN L. RODGERS
Chief, Advanced Research in Energy
Storage Office

FOR THE DIRECTOR

[illegible]

REPORT DOCUMENTATION PAGE

Form Approved
OMB No. 0704-0188

1. AGENCY USE ONLY (Leave blank)	2. REPORT DATE	3. REPORT TYPE AND DATES COVERED
	Jan 1991	Final for 8705-8908

4. TITLE AND SUBTITLE
Quantum Chemical Studies of Candidate High Energy Density Material Compounds

5. FUNDING NUMBERS
F04611-87-X-0059
F04611-88-C-0067
PEN: 62302F
JON: 573000VJ

6. AUTHOR(S)
George F. Adams and Cary F. Chabalowski

7. PERFORMING ORGANIZATION NAME(S) AND ADDRESS(ES)
US Army Ballistic Research Laboratory
Attn: SLCBR-DD-T
Aberdeen Proving Ground MD 21005-5066

8. PERFORMING ORGANIZATION REPORT NUMBER

9. SPONSORING / MONITORING AGENCY NAME(S) AND ADDRESS(ES)
OLAC, Phillips Laboratory (AFSC)
OLAC PL/LSX
Edwards AFB CA 93523-5000

10. SPONSORING / MONITORING AGENCY REPORT NUMBER
AL-TR-89-055

11. SUPPLEMENTARY NOTES
Monitoring organization formerly named the Astronautics Laboratory (AFSC).
Work unit accession number: 343750

12a. DISTRIBUTION / AVAILABILITY STATEMENT
Approved for Public Release; Distribution Unlimited.

12b. DISTRIBUTION CODE

13. ABSTRACT *(Maximum 200 words)*

This report describes the development and application of *ab initio* quantum chemical methods that are especially relevant to the study of high-energy density materials species. Two major quantum chemical program systems, MESA and BROOKLYN, have been developed during the tenure of this research effort. Each of these development efforts was performed, in large part, at the Ballistic Research Laboratory (BRL) and The Johns Hopkins University. Here we report the results of quantum chemical studies on molecular systems that are thought to be relevant to high-energy density material research. These include detailed descriptions of the electronic excited states of He_2, the energy loss mechanisms for the He^* -H_2 systems, detailed structural studies data for a series of triborane species, an analysis of the stability of four-atom metal clusters with molecular formulae B_2Li_2 and B_2Be_2, and a preliminary theoretical study of the energy storage potential of hydrogen halide-doped rare gas solids.

14. SUBJECT TERMS
HEDM, B_3H_3, B_2Be_2, B_2Li_2, *ab initio*, He^*, He_2, Quantum Chemistry, Spin States, Molecular States, Molecular Properties

15. NUMBER OF PAGES

16. PRICE CODE

17. SECURITY CLASSIFICATION OF REPORT	18. SECURITY CLASSIFICATION OF THIS PAGE	19. SECURITY CLASSIFICATION OF ABSTRACT	20. LIMITATION OF ABSTRACT
UNCLASSIFIED	UNCLASSIFIED	UNCLASSIFIED	SAR

INTENTIONALLY LEFT BLANK.

TABLE OF CONTENTS

INTENTIONALLY LEFT BLANK.

LIST OF FIGURES

INTENTIONALLY LEFT BLANK.

LIST OF TABLES

INTENTIONALLY LEFT BLANK.

1. INTRODUCTION

The timely study of candidate species for high-energy density applications requires access to efficient and sophisticated quantum chemical techniques implemented on advanced high-performance computers. This report documents the development of quantum chemical methods particularly well-suited to the study of metastable materials and molecular states, and the application of these techniques to describe the stability and properties of a number of novel chemical systems. While much of the work was performed at the Ballistic Research Laboratory (BRL), we have enjoyed the expert assistance of our collaborator, Dr. David Yarkony, of The Johns Hopkins University, and the skills of our former co-worker, Dr. Byron Lengsfield III, now at the Lawrence Livermore Laboratory. Portions of the work described in this report were performed during the time that Dr. Lengsfield was at the BRL.

Throughout the term of this research, two complementary, and sometimes competing, efforts were maintained. Our first effort successfully attempted to develop and demonstrate efficient quantum chemical techniques for the precise prediction of the existence and properties of metastable states and species. Additionally, we performed quantitative theoretical studies on a number of candidate metastable species, including the ill-fated tetrahydrogen molecule.

Initially these molecules included proposed hypervalent compounds such as NH_4 and CH_5, a series of hydrogen-rich boranes, and excited states of the helium dimer. The latter computations were required for the dynamical studies performed by the Chemical Dynamics Corporation. As the program evolved, we eliminated some of these species from active consideration and added others deemed more relevant to the High-Energy Density Materials (HEDM) program. The most important additions were the tetratomic low-molecular weight clusters of lithium, beryllium, and boron, and the interaction of hydrogen halides with rare gas atom clusters. The following sections summarize the results obtained for each of these efforts.

2. QUANTITATIVE STUDIES ON CANDIDATE HEDM SPECIES

2.1 Borane Compounds. At the onset of this project, several groups were investigating the possibility of energy storage in small boron hydride compounds. Since we had already begun a study of the structures and energy storage in the B_1 and B_2 boranes, an extension of systems of interest in

HEDM applications seemed natural. While identification of the thermally stable isomers of the B_nH_m species is important, it is equally important to determine the heat of formation of these species. In our previous work (Adams and Page, to be published), we had used perturbation theory calculations to determine the relative energies and heats of formation for 13 boranes. For the HEDM project, we began with the closed-shell triborane isomers, B_3H_3, B_3H_5, and B_3H_7. We have also revisited B_2H_2 in order to provide complementary data to recent CompleteActive Space Self-Contained Field (CASSCF) results obtained by Lengsfield (private communication). The discussion of triborane (Montgomery and Michels, private communication), a compound containing three boron and three hydrogen atoms, is deferred to the next paragraph, since that compound provides an interesting challenge to theorists. Here we describe the results for the larger triboranes.

The structures of two stable B_3H_5 isomers were determined. One is a classically bonded structure with BH_2 groups. The other structure has two bridge hydrogens. Cartesian coordinates are given in Table 1. While one may imagine additional isomers for this molecular formula, we believe that these two conformers are probably the lowest energy forms. Unfortunately, it is unlikely that these thermally stable isomers are viable energy storage species for HEDM applications because of the propensity for small boranes to condense. Similarly, while we have also located two stable isomers of B_3H_7, there seems to be little application for such species given the objectives of this program. Consequently, after discussions with the staff at the Astronautics Laboratory, Edwards Air Force Base, CA, it was decided to discontinue the study of the borane isomers, focusing instead upon species that seemed more suited to the objective of increased specific impulse. The exception is triborane (Montgomery and Michels, private communications), which we discuss at length in the following section.

2.2 Isomers of B_3H_3. The initial studies on triborane were those of Montgomery and Michels (private communication), reported at the May 1987 HEDM review. They had attempted to locate an isomer of this chemical formula that possessed D_{3h} symmetry. As part of another study, we had located a structure with C_{2v} symmetry that had a significantly different geometric structure than that proposed by Montgomery and Michels. Schematics of the two isomers are shown in the Table 1. Montgomery and Michels had noted that their calculations predicted that the D_{3h} isomer was not thermally stable, possessing negative second derivatives. Those calculations, like our initial calculations, employed Self-Contained Field (SCF) gradient methods with double zeta plus polarization quality basis sets. Subsequently, we initiated a series of calculations to locate a C_{2v} isomer similar to the D_{3h} isomer described by Montgomery and Michels.

Table 1. Cartesian Coordinates of B_3H_5 Isomers (au)

	X	Y	Z
Classical triborane [3]			
B_1	0.0000	0.0000	0.0000
B_2	-1.4205	2.8361	0.0000
B_3	-1.4205	-2.8361	0.0000
H_1	2.2675	0.0000	0.0000
H_2	-1.9380	3.8941	-1.9234
H_3	-1.9380	-3.8941	-1.9234
H_4	-1.9380	3.8941	1.9234
H_5	-1.9380	-3.8941	1.9234
Nonclassical triborane [3]			
B_1	0.0000	0.0000	0.0000
B_2	-2.6823	1.6520	0.0000
B_3	-2.6823	-1.6520	0.0000
H_1	2.2254	0.0000	0.0000
H_2	-3.7538	0.0000	-1.7202
H_3	-3.7538	0.0000	1.7202
H_4	-3.8708	3.5501	0.0000
H_5	-3.8708	-3.5501	0.0000

By reducing the symmetry to C_{2v}, a thermally stable structure for this "loose" isomer was predicted, yielding two stable isomers of this chemical formula.

As occurs often in quantum chemical studies of boron compounds, the SCF computations resulted in more negative molecular orbital eigenvalues than electron pairs. This suggests that a single reference wavefunction may be inadequate for these molecules. To resolve this issue, we extended the scope of the calculations on these systems to include correlation energy effects, performing both many-body perturbation theory and CASSCF calculations on these isomers. The CASSCF calculations were done using the Molecular Electronic Structure Applications (MESA) electronic structure theory codes, while the second-order perturbation theory results were obtained using the Cambridge Analytic Derivatives Package (CADPAC) (Amos and Rice 1988). In this study, we determined the structure and second derivatives for each of the isomers. The internal coordinates and second derivatives predicted for the "tight" isomer are summarized in Table 2, while the data for the "loose" isomer are presented in Table 3. The internal coordinate, R_1, describes the bond between the apex boron atom and the hydrogen bonded to it, while R_2 represents the boron-boron bond length. In the case of the tight isomer, the distance between the symmetry related boron atoms is less than the distance between those atoms and the apex boron.

The tables represent the results for all levels of electronic structure theory used in this study. The results for the tight isomer indicate the challenge presented in the study of these novel systems. All three computational methods predict similar bond lengths. The methods disagree dramatically in the prediction of the bond angle formed by the symmetric hydrogen, the symmetric boron, and the apex boron atoms. Further, the second derivatives obtained in the MP2 calculation predict that the structure is a transition state. The CASSCF calculation correlated four electrons in seven orbitals. While the predicted structure is characterized as a minimum on the potential energy surface, the HBB bond angle is especially low. This calculation used starting orbitals obtained from configuration interaction (CI) natural orbital calculations.

Here we digress to comment on the CASSCF calculations. We chose the active space to comprise those orbitals needed to account for four electrons. To correlate more electrons would have required far more computational resources than we can access. In the case of the tight structure, we used a four-electron-in-seven orbital calculation, while the looser structure required a four-electron-in-six orbital calculation, basing our selection upon the natural orbital eigenvalues (Table 4). The present

Table 2. Internal Coordinates and Frequencies for Triborane [3]

	SCF	MP2	4-in-6 CASSCF
R_1	1.1808	1.1781	1.1778
R_2	1.5450	1.5354	1.5451
R_3	1.1761	1.1782	1.1765
A_1	136.9	140.5	138.4
A_2	170.1	168.8	168.3
τ_1	180.0	180.0	180.0
Harmonic Frequencies			
	237.5	137.1	230.8
	339.2	364.4	401.6
	407.3	518.1	473.1
	733.8	683.1	660.5
	819.0	791.0	793.2
	884.5	796.5	863.6
	901.8	905.3	891.9
	1142.6	1086.6	1093.7
	1177.4	1198.8	1191.9
	2805.7	2805.6	2791.0
	2880.1	2833.0	2854.4
	2889.1	2850.1	2852.9
Energy (h)			
	-75.653292	-75.936285	-75.70674

Table 3. Internal Coordinates and Frequencies for Triborane [3]

	SCF	MP2	4-in-7 CAS
R_1	1.1756	1.178	1.1765
R_2	1.7070	1.676	1.7363
R_3	1.1800	1.1874	1.1783
A_1	154.6	153.9	154.9
A_2	103.7	96.3	50.1
τ_1	0.0	0.0	0.0
Harmonic Frequencies (cm^{-1})			
	190.6	-499.7	198.4
	230.6	433.4	313.4
	247.2	496.6	360.6
	637.3	539.3	597.5
	681.5	656.5	623.2
	813.0	775.8	798.8
	842.6	794.1	801.1
	1090.6	1088.9	1018.6
	1418.8	1340.4	1382.4
	2822.6	2747.8	2831.6
	2866.6	2793.8	2863.1
	2882.6	2838.5	2875.9
Energy (h)			
	-75.65001	-75.94004	-75.715729

Table 4. Natural Orbital Ergenvalues for Triborane [3]

Orbital #	Eigenvalues
4	1.9779
5	1.9720
6	1.9719
7	1.9649
8	1.9517
9	1.9385
10	0.0405
11	0.0318
12	0.0183
13	0.01648
14	0.01643

CASSCF calculations should be superior to previous calculations described in progress reports, since the inclusion of more "virtual" natural orbitals provides a more complete basis to describe the correlation of four electrons. As noted most recently by Page (1989), more approximate CASSCF calculations, those that truncate the correlation space, often predict second derivatives that are too low. This phenomenon may explain the negative second derivative obtained in our earlier studies. Furthermore, it seems pertinent to suggest that the MP2 results for the tight isomer may be due to the limited degree of correlation employed in those studies. In any event, more accurate calculations indicate that both structures are stable species rather than transition state structures.

In addition to the isomers described above, we have determined structures and second derivatives for two additional isomers of triborane (Montgomery and Michels, private communication). The data describing these isomers are summarized in Tables 5 and 6. The four isomers, taken together, contain a number of BB and BH bond types, providing model systems for the development of bond-additivity parameters as needed for the development of a rationale thermochemistry for this class of compounds.

2.3 Isomers of B_2Be_2 and B_2Li_2. Inclusion of metals in propellant formulations is a common practice that generally provides increased energy output. The search for novel, high-energy density materials includes efforts to find new sources of low atomic weight metals to provide high-energy release and high specific impulse. Lammertsma, et al. (private communication), in a research effort supported by the HEDM program, have reported on a number of tetratomic species that display novel bonding. Among the many molecules studied were tetratomic clusters with formulae B_2Be_2 and B_2Li_2, species expected to provide outstanding energy release when combined with suitable oxidizers. Specifying the energy release requires knowledge of the heat of formation for these species. The Lammertsma project provided structure and second derivative information using both SCF and second-order perturbation theory methods. After discussion with Lammertsma and the project monitors, we agreed to investigate several of these isomers using both higher order perturbation theory and CASSCF methods. Our goals were to verify the stability of the individual molecules and to provide an estimate of the heats of formation of these species. To this end, we have repeated the determination of SCF structures for four of the metal isomers and completed extended basis set, third-order, perturbation theory calculations for the tetragonal isomers. The latter calculations provide the information enabling us to predict accurate atomization energies using a technique developed at this laboratory (Adams, Gallo, and Page 1989). In addition, we have completed a series of CASSCF calculations that provide

Table 5. Internal Coordinates and Frequencies for Triborane [3]

	SCF	MP2
R1	1.629	1.597
R2	1.544	1.564
R3	1.171	1.174
R4	1.194	1.196
A1	120.7	120.7
Harmonic Frequencies		
	211.1	174.6
	223.5	189.9
	636.2	553.3
	683.1	604.3
	761.1	756.4
	852.8	816.1
	994.7	931.5
	1228.5	1150.7
	1433.2	1387.0
	2669.8	2636.4
	2746.4	2727.1
	2923.4	2880.3
	-75.645046 h	-75.89829 h

Table 6. Internal Coordinates and Frequencies for Triborane [3]

	SCF	MP2
R1	1.6731	1.597
R2	1.1925	1.193
R3	1.7803	1.564
R4	1.2008	1.201
R5	1.1962	1.196
A1	121.6	122.0
A2	126.6	126.8
A3	118.7	119.9
A4	121.1	120.6
T1	90.	90.
T2	-90.	-90.
T3	-90.	-90.
Harmonic Frequencies		
	213.7	188.4
	308.4	277.1
	483.9	427.0
	705.3	620.1
	716.4	693.7
	792.5	757.3
	974.4	961.3
	1101.1	1045.3
	1249.8	1181.7
	2659.8	2625.2
	2681.4	2649.7
	2759.3	2718.7
	-75.583948 h	-75.841326 h

additional evidence that a number of these isomers are thermally stable species. We present first the perturbation theory data, and then the data obtained using the multiconfiguration theory techniques.

2.4 Structure and Energy Content of Tetratomic Metal Clusters. Using the CADPAC system of quantum chemical programs (Amos and Rice 1988), we have determined optimized structures of the rhombic and tetragonal isomers of B_2Li_2 and B_2Be_2, using a 6311G* basis set (Krishnan et al. 1980). These SCF and MP2 results are summarized in Tables 7 and 8. The computed harmonic frequencies for the four isomers predict each to be thermally stable. The energy separations predicted for the isomers are relatively small for both compounds for both SCF and MP2 results. The MP2 data predicts that the rhombic structure is the more stable B_2Li_2 isomer, whereas the tetragonal structure is favored for B_2Be_2. The structures for the B_2Be_2 isomers appear to differ from those reported by Lammertsma (private communication), perhaps because we used a larger basis set to perform the optimization. It is interesting to note that our calculations predict that the boron atoms have partial negative charges, whereas the smaller basis set studies have the excess electrons on the beryllium atoms. In the case of B_2Li_2, both sets of calculations have the excess electrons on the boron atoms. The structural predictions obtained in the two studies are in good agreement with one another, except that the lithium-lithium separation for the rhombic structure is predicted to be shorter in the MP2 model than in the SCF model. Interestingly, this difference does not result in dramatically changed vibrational frequencies.

To estimate the heats of formation, we utilize a perturbation theory technique that yields excellent estimates of molecular atomization energies at moderate computational cost. While the technique is limited in application to sigma-bonded molecules, tests to date indicate that the results are accurate. The method rests upon the use of extended basis sets in theoretical studies. In a number of studies on the computation of molecular properties, Handy (1986) and co-workers demonstrated that excellent agreement between theory and experiment were obtained using low levels of electron correlation. The computational savings are substantial. Related to these studies were calculations by Carter and Goddard (1988) that used the efficient generalized valence bond-configuration interaction (GVB-CI) method with extended basis sets to predict with accuracy the singlet-triplet splitting in the methylene radical. Our technique employs the isogyric analysis method suggested by Pople et al. (1983), wherein atomization energies are derived by comparison with the known atomization energy of the H_2 molecule. Our data shows that extended basis set third-order perturbation theory, when used with the isogyric technique, predicts atomization energies for sigma-bonded systems that are as accurate as

Table 7. Isomers of B_2Li_2: Structural Parameters and Frequencies

	SCF	MP2		SCF	MP2
R_{BLi}	2.1870	2.1595	R_{BLi}	2.2406	2.1804
R_{BB}	1.5355	1.5417	R_{BB}	1.5436	1.5146
α_{BBLi}	69.405	69.084	R_{LiLi}	3.5017	3.1700
γ_{LiBBLi}	180.0	180.0	α_{BBLi}	69.850	69.67
			α_{LiBLi}	102.78	93.26
			γ_{LiBBLi}	-112.686	101.648
Harmonic Frequencies (cm-1)					
	244.2	258.6		133.7	184.3
	254.4	501.2		288.7	382.2
	518.3	517.8		335.9	455.1
	519.8	623.4		492.3	534.1
	609.6	1022.5		549.3	602.4
	1129.2	1163.4		1159.9	1177.0
Energy (hartrees)					
	-64.06446	-64.36478		-64.07829	-64.35211

Table 8. Isomers of B_2Be_2: Structral Parameters and Frequencies

	SCF	MP2		SCF	MP2
R_{BBe}	2.0078	1.7996	R_{BBe}	2.2406	1.7919
R_{BB}	1.7108	1.5407	R_{BB}	1.5436	1.5449
α_{BBBe}	55.112	64.65	R_{BeBe}	3.5017	2.0891
γ_{BeBBBe}	180.0	180.0	α_{BBBe}	64.46	64.46
			α_{BeBBe}	71.31	71.31
			γ_{BeBBBe}	±80.48	±80.48
Harmonic Frequencies					
	264.5			405.5	425.6
	413.1			514.0	604.4
	441.6			658.4	681.9
	771.8			853.1	813.7
	911.9			875.9	817.0
	1052.1			1131.7	1136.8
Energy (hartrees)					
	-78.35004	-78.73456		-78.39660	-78.76709

those determined using full-fourth-order perturbation theory calculations. In the case of B_2Be_2, the isogyric equation for the atomization process is

$$B_2Be_2 + 2\,H \rightarrow 2\,B + 2\,Be + H_2.$$

Table 9 contains both the third-order perturbation theory energy obtained in the extended basis set calculation and the predicted atomization energy for the two tetragonal isomers. Using the "established" heats of formation of the lithium, beryllium, and boron atoms, the heat of formation for the tetragonal isomers may be deduced. Using heat of formation data from the JANNAF thermochemical tables (not always a reliable source), the heats of formation given in Table 10 are predicted.

3. CASSCF STUDIES OF CLUSTER STRUCTURES

The description of the low molecular weight metal clusters given in the previous section was based upon the application of theoretical methods that assumed the wavefunction could be well-described by a single-configuration wavefunction. That this assumption is questionable can be deduced by noting that the coefficient of the largest contribution to the general wavefunction, also known as c(0), is less than 0.95 for all four structures previously described. When this is the case, it is generally regarded as prudent to reexamine the molecular system using a more general method. In most cases, the choice is multiconfiguration, self-consistent field theory. We have used the CASSCF capabilities of MESA to generalize the study of the B_2Be_2 and B_2Li_2 molecules.

As we noted in the discussion of B_3H_3, the definition of the active space is not a precise process. Those results demonstrated the need to develop a consistent approach to definition of the active space. Unfortunately, it is not clear that such a definition can be made. The metal cluster computations emphasize the need to devise a consistent, active space paradigm. While we have investigated both the boro-lithium and boro-beryllium tetramers, we have been more successful in compiling information on the B_2Li_2 isomers. It is not clear, at this point, why the computations on the boron-beryllium isomers have led to numerical difficulties in so many instances.

The data presented in Table 11 hints at the need to employ post-Hartree-Fock methods. With a double zeta plus polarization basis set, the structure predictions obtained using SCF theory differ

Table 9. B_2Li_2 and B_2Be_2 Energetics

	B_2Li_2	B_2Be_2	B	Be	Li
Electronic Energy	-64.30128	-78.82698	-24.595	-14.418	-7.432
Zero Point Energy (kcal m^{-1})	4.7	6.4			

Table 10. Extended Basis Set Results: Tetragonal Isomers

	MP3 Energy (h)	Atomization Energy (h)	ΔH_f^{298}
B_2Be_2	-78.826985 h	0.35285 h	194.4 kcal m^{-1}
B_2Li_2	-64.301286 h	0.34892 h	119.0 kcal m^{-1}

Table 11. Results for B_2Li_2: Tetragonal Structure

Optimized Z-matrix Parameters:		
	SCF	CASSCF (6-in-6)
R_{LiLi}	3.54775 b	3.89813 b
R_{LiB}	2.69119 b	2.19152 b
R_{BB}	1.55068 b	1.55622 b
ζ_{LiLiB}	38.327	27.201
ζ_{LiBB}	69.947	69.205
ζ_{BBLiLi}	62.501	42.371
Frequency Predictions:		
ν_1	139.4	45.0
ν_2	280.4	274.9
ν_3	327.2	472.6
ν_4	481.9	507.6
ν_5	536.9	609.0
ν_6	1140.0	1119.7

dramatically from the parameters determined using a six-electron-in-six orbital complete active space (CAS) technique. While these results emphasize the importance of including electron correlation effects to obtain consistent results, it is not obvious that the CAS data is closer to "reality" than the SCF results. The extremely low frequency predicted by the six-in-six calculation suggests that a larger active space should have been used in the calculation. The data summarized in Table 12 supports this conclusion. Using both techniques on the rhombic isomer of B_2Li_2, we find that the structures are predicted to be similar. The lowest frequency predicted by the CASSCF technique is low. While electron correlation effects have been included, it is not clear that we have obtained "better" results. Finally, the frequency calculations summarized in Table 13 provide, we believe, clear indications that great care must be exercised in selecting the active space. The first two columns contain the frequency predictions obtained for B_2Li_2 using the CASSCF structure. Expanding the calculation to include eight orbitals in the active space results in a dramatic increase in the lowest frequency. On the other hand, if we perform a similar series of computations using the larger 6-311G* basis set, neither a six-in-eight nor an eight-in-eight calculation predicts the new structure to be thermally stable. Note that the eight-in-eight calculations value of the lowest frequency is lower than that of the six-in-eight calculation. While the data presented is limited, it seems clear that the selection of that active space is crucial obtaining reliable structural and force constant information for these species. In fact, it may be better to reduce the number of electrons correlated in order to guarantee that the active space is large enough.

We can summarize our results to date succinctly. In spite of the apparently contradictory results, it is likely that both the tetragonal and rhombic isomers of B_2Li_2 are thermally stable species. We are more certain that the rhombic isomer of B_2Be_2 is a thermally stable species, but we note that both Lammertsma's study and our own have identified a distorted rhombic structure that is a transition state. Thus, the rhombic B_2Be_2 is not necessarily dynamically stable. While we are not entirely pleased with the progress of this portion of the work, the information available now leads us to cautious optimism with respect to the usefulness of these molecules. In particular, it seems prudent to determine the stability of the B_2Li_2 isomers with respect to external perturbations, such as proximity of a second isomer or an oxidizing molecule. These perturbations can be investigated using CASSCF-based surface walking techniques. This information, coupled with better CASSCF calculations on the monomer clusters, should provide data of sufficient accuracy to determine the viability of these species as HEDM.

Table 12. Results for B_2Li_2: Rhombic Structure

Optimized Z-matrix Parameters:		
	SCF	CASSCF (6-in-6)
R_{BB}	1.53551 A	1.55480 A
R_{LiB}	2.20513 A	2.18360 A
R_{BLi}	2.20513	2.18360
ζ_{BBLi}	69.6247	69.1443
ζ_{BBLi}	69.6247	69.1443
τ_{BBLiLi}	180.0	180.0
Frequency Predictions:		
ν_1	229.1	12.8
ν_2	336.3	242 3
ν_3	508.2	493.5
ν_4	513.0	514.5
ν_5	609.5	619.4
ν_6	1132.3	1123.9

Table 13. CASSCF Frequencies (cm^{-1}) for Rhombic B_2Li_2

	DZP		6311G*	
	6-in-6	6-in-8	6-in-8	8-in-8
ν_1	12.8	132.4	-54.9	-115.5
ν_2	242.3	250.7	254.9	250.0
ν_3	493.5	496.5	497.5	489.4
ν_4	514.5	519.9	519.9	517.8
ν_5	619.4	621.4	618.2	619.0
ν_6	1123.9	1124.8	1128.9	1130.0

4. H_3 COMPLEXES, INCLUDING TETRAHYDROGEN

Ab initio Multi-Configuration Self-Consistent Field (MCSCF) calculations were performed on the tetrahydrogen species suggested by Nicolaides, Theodorapoulis, and Petsalakis (1984). Since our MCSCF techniques include the ability to compute first and second derivatives using analytic formulas, we are able to efficiently search potential energy surfaces for stationary points. It has been proposed that tetrahydrogen possesses a metastable $^1A_1$ state that can dissociate to two stable hydrogen molecules. The state is postulated to be formed at small intermolecular separations as a result of the avoided crossings of two singlet states. Extensive MCSCF calculations were performed to characterized the molecule in the region described by Nicolaides et al. in their work. We find that there are no minimum energy points in this region on the lowest energy hypersurface. The stable point on the C_{3v} (pyramidal) surface is characterized by two negative eigenvalues of the force constant matrix. Using reaction path, surface walking algorithms, we have followed the motion of the hydrogen atoms as they dissociate from the C_{3v} stable point to form the two hydrogen molecules.

We have also investigated the upper state generated by the avoided crossing. The upper surface arises from an E state at the C_{3v} geometries investigated by Nicolaides et al. The fact that this surface arises from an *E* state has important implications in light of earlier studies of this system. First, the system distorts so that the minimum is no longer at a C_{3v} geometry, and, second, nuclear motion that preserves the C_{3v} geometry will not couple to these states via first-order nonadiabatic coupling which is important near the minimum of the C_s state.

A series of self-consistent field calculations were performed seeking stable complexes with the H_3 molecule. We investigated the following pairs:

fluorine atom, oxygen anion
fluorine cation, oxygen atom,

as well as an oxygen atom sandwiched between two trihydrogen rings. The calculations were performed using SCF and CAS-MCSCF methods at a variety of symmetric geometries.

The series of compounds is of interest since one expects that a combination of a stable molecular ion with another stable species may lead to the formation of a stable complex. Since the specific

impulse of a hydrogen-rich species would be higher that of a typical energetic material, the desire to find such a species seemed obvious in the context of the HEDM research effort.

The atomic basis set used in the studies included the standard double zeta plus polarization basis set of Dunning, augmented with a Rydberg s-function on the hydrogens and s- and p-functions on the first row atoms.

For the H_3O^- and H_3F isoelectronic molecules, the distance between the equilateral triangle of hydrogen atoms, with internuclear separation r, and the first row atom was varied. The H-H separation was selected to be 1.6 au, and the separation between the midpoint of the triangle and the first row atom was varied between 2.8 and 3.0 au. The variation yielded a near-minimum for the C_{3v} structure. Both of the near minimum structures had negative force constant eigenvalues corresponding to distortion that broke the C_{3v} symmetry. Both structures corresponded to charge transfer states.

Similar, near-C_{3v} structures were obtained for the other complexes. Again, the C_{3v} structures were characterized by negative eigenvalues of the force constant that corresponded to motions breaking the C_{3v} symmetry.

We conclude that it is unlikely that one will locate a stable hypervalent complex comprising H_3 and a low molecular weight atom.

5. SPIN FORBIDDEN TRANSITION LIFETIMES

Among methods to store energy, one approach may be the production of long-lived, excited electronic states. The helium diatomic $a^3\Sigma_u^+$ state is a possible candidate, since the radiative decay process, $a^3\Sigma_u^+ \rightarrow X^1\Sigma_g^+$, is a spin-forbidden transition and is therefore expected to be very slow. Experimentally, the generation of neutral excited state helium atoms or molecules in a liquid helium bath via collisions with alpha particles was initially reported by Surko and Reif (1968a). Calvani, Maraviglia, and Messana (1972), generating the neutral entities from an alpha source, set a lower limit of 0.1 sec on its natural lifetime (τ). A more recent experimental study by Mehrotra, Mann, and Dahm (1979) concluded that the neutral excited species was the molecular $a^3\Sigma_u^+$ state in He_2. This is reported to be the lowest energy excited electronic state in He_2 and the lowest bound state (the $X^1\Sigma_g^+$ ground state is essentially repulsive). They predict from their data a lower bound on the natural

lifetime of 10 sec in the liquid medium. In view of the large difference (a factor of 100) predicted by the two experiments (Mehrotra, Mann, and Dahm 1979; Yarkony 1987) for the lower limit in τ, an estimate of the lifetime using high-quality *ab initio* calculations is in order.

5.1 Methods. This study calculates τ for the spin-forbidden transition, $a^3\Sigma_u^+ \rightarrow X^1\Sigma_g^+$, for He_2 is the gas phase using state-averaged MCSCF plus CI to generate the appropriate zeroth-order wavefunctions. In order to calculate this spin-forbidden process, spin-orbit (S-O) interactions are calculated with a manifold of exited states via matrix elements over configuration-state-functions (CSFs) using the microscopic Breit-Pauli Hamiltonian. This newly implemented method (Yarkony 1987) incorporates the application of the symbolic matrix method of Liu and Yoshimine (1987) into the formation of the S-O matrix elements. In addition, the calculation is further simplified by solving directly for the first-order correction, Ψ^1, to the state wavefunction by obtaining directly Ψ as an eigenvector that results from diagonalizing a set of linear equations which contain matrix elements over CSFs.

In contrast, the usual representation for the first-order correction, $\Psi^1(I)$, due to S-O effects is

$$\Psi^1(I) = \sum_L^{\infty} \frac{\langle \Psi_J^o | \tilde{H}^{so} | \Psi_I^o \rangle}{(E_J^o - E_I^o)} \Psi_J^o. \tag{1}$$

The summation over the L electronic states is, in principle, infinite. One often used approach to solving for $\Psi^1(I)$ is to calculate explicitly the wavefunctions for a relatively small number of excited states thereby drastically truncating L. This might cause one to miss important contributions to $\Psi^1(I)$ from the omitted states.

The "omitted states" problem can be significantly reduced by the method used in this study wherein one solves for Ψ^1 directly from

$$(\tilde{H}^o - E_I)\,\Psi_I^1 = \tilde{H}^{so}\Psi_I^o \tag{2}$$

with $\tilde{H}^o$ being the non-relativistic Hamiltonian. Equation 2 can be transformed into matrix form as

$$(H^o - E_I)\,V_I^1 = -\tilde{H}^{so}C^I \tag{3}$$

where it must be emphasized that H^o and H^{so} are matrices with elements formed over CSFs, NOT over eigenstates. The vectors V^I and C^I are defined as the coefficients for the first- and zeroth-order parts of Ψ_I:

$$\Psi_I^o = \sum_i C_i \phi_i(\kappa)$$

$$\Psi_I^1 = \sum_j V_j \phi_j(\kappa') . \tag{4}$$

The κ and κ' label the spatial symmetries to which the CSFs belong, in general $\kappa \neq \kappa'$. Equation 3 forms a large set of linear, inhomogeneous equations which are solved to obtain V_j by a variant of the method suggested by Pople et al. (1983).

The natural lifetime is then dependent upon the electric transition dipole moment for the electronic transition $a^3\Sigma_u^+ \rightarrow X^1\Sigma_g^+$. This is finally represented as the sum of singlet and triplet contributions:

$$\mu_1 = \langle \Psi^o(a^3\Sigma_u^+) | \mu_{+1} | \Psi^1(^3\Pi_g) \rangle + \langle \Psi^1(^1\Pi_u) | \mu_{+1} | \Psi^o(X^1\Sigma_g^+) \rangle \tag{5}$$

which are matrix elements in terms of zeroth- and first-order corrections to the wavefunctions. The μ_1 values were then used in a vibrational analysis to include the effects of nuclear motion which allows one to predict vibrational energy levels and make direct comparison with experimental values for lifetimes of the excited state vibrational levels.

5.2 Details of Calculations. The gaussian-type basis set is essentially that used by Sunil et al. (1983) in an earlier theoretical study on excited states of He_2 with two exceptions. A single primitive p-function has been added with it's exponent optimized to give the lowest CI energy for the $F^1\Pi_u$ at the He-He distance r=2.00 au. In addition, the orbital exponent for the more diffuse d-function was changed to be consistent with a basis set used in an earlier study on He_2 in this laboratory (Konowalow and Lengsfield 1987). The final basis set consists of (10s,6p,2d) primitives contracted to [7s,5p,2d] atomic orbitals (AO), for a total of 34 basic functions per atom.

The spatial symmetry is chosen to be the D_{2h} point group for all the calculations performed. The State-Averaged Multi-Configuration Self-Consistent Field (SAMCSCF) is of the CAS-type wherein the four electrons are distributed in all possible ways amongst the lowest three molecular orbitals (MO) from irreducible representations $A_g(\sigma_g)$ and $B_{1u}(\sigma_u)$, and the lowest MO from $B_{2u}(\pi_{uy})$, $B_{3u}(\pi_{ux})$, $B_{2g}(\pi_{gx})$, and $B_{3g}(\pi_{gy})$, consistent with space and spin symmetry restrictions. The state-averaged

energy is then optimized including the states $X^1\Sigma_g^+$, $a^3\Sigma_u^+$, $b^3\Pi_{gx}$, $b^3\Pi_{gy}$, $F^1\Pi_{ux}$, and $F^1\Pi_{uy}$. The MOs obtained from the SAMCSCF were then used as the basis set for the CI. The CSFs used in the SAMCSCFs were then used as reference CSFs in the CI, from which all single and double excitations where performed.

5.3 Results. The main configuration for each of the four states, as found in the CI at r=2.00, is $X^1\Sigma_g^+$: $1\sigma_g^2 1\sigma_u^2$, $a^3\Sigma_u^+$: $1\sigma_g^2 2\sigma_g 1\sigma_u$, $b^3\Pi g$: $1\sigma_g^2 1\sigma_u 1\pi_u$, $F^1\Pi u$: $1\sigma_g^2 1\sigma_u 1\pi_g$. Table 14 compares the molecular constants for the four states of interest as predicted by a vibrational analysis on the potential energy curves (PEC) from this study and experiment. The theoretical D_e values are calculated as the difference in energy, $E(r_e)$ - E(r=40 bohr). As can be seen, the calculated r_e, ω_e, T_e, and D_e for all four states vary from experiment by no more than 1%. These states seem well described.

PECs for the four states are shown in Figure 2. The $a^3\Sigma_u^+$ and $F^1\Pi_u$ are found to have local maxima in their PECs as the molecule goes toward dissociation. Various experimental and theoretical estimates have been made on the height and location of these humps, and a summary of these predictions (including the results from this study) can be found in Table 15. These calculations give the barrier size (i.e., ΔE=E[max] - E[dissociation]) and location of the $a^3\Sigma_u^+$ to be ΔE=1.56 kcal/mol and r(He-He)=2.7 Å, respectively. For the $F^1\Pi_u$ state, the barrier height is ΔE=10.9 kcal/mol at the internuclear separation, r(He-He)=1.79 Ångs. The $F^1\Pi_u$ values vary somewhat from earlier estimates (see Table 14).

The first-order S-O corrections to the $X^1\Sigma_g^+$ and $a^3\Sigma_u^+$ states arise from interactions of these zeroth-order wavefunctions with the $^3\Pi_g$ and $^1\Pi_u$ state manifolds, respectively, as defined by the CSF expansions for these Π spaces. The magnitude of the S-O perturbation of the $a^3\Sigma_u^+$ by the entire $^1\Pi_u$ manifold (as spanned by this CSF space) is plotted in Figure 2 and labeled Curve A. Curve B in Figure 1 represents the first-order S-O interaction between the $a^3\Sigma_u^+$ zeroth-order wavefunction and only the lowest energy state of $^1\Pi_u$ symmetry, i.e., the $F^1\Pi_u$. This gives a first-order correction, $\Psi^1(a^3\Sigma_u^+)$, equivalent to setting L=1 in the summation of Equation 1. Therefore, the difference in magnitude between Curves A and B should reflect the contribution to the first-order perturbation correction, $\Psi^1(a^3\Sigma_u^+)$, that is missed by truncating the summation in Equation 1 to simply L=1. The analogous information is plotted in Figure 2 for the $X^1\Sigma_g^+$ state perturbed by the $^3\Pi_g$ manifold (Curve A) or only the $b^3\Pi_g$ state (Curve B).

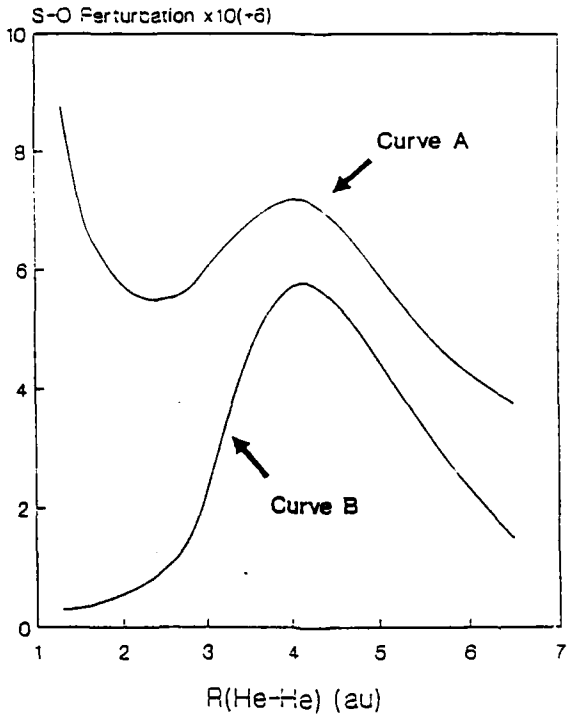

Figure 1. First-Order Contribution to the S-O Perturbant of the $a^3\Sigma_u^+$ by the $^1\Pi_u$ State Manifold (Curve A) and by the $F^1\Pi_u$ State (Curve B) as a Function of Internuclear Separation.

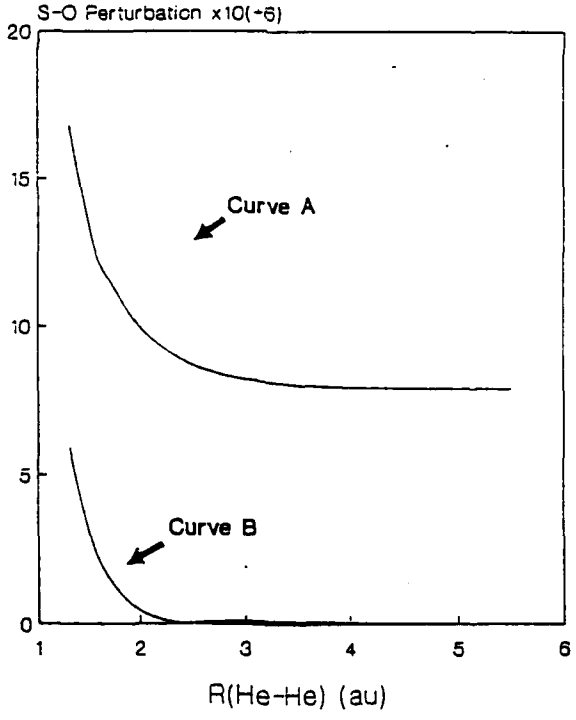

Figure 2. First-Order Contribution to the S-O Perturbation of the $X^1\Sigma_g^+$ by the $^3\Pi_g$ State Manifold (Curve A) and by the $b^3\Pi_g$ State (Curve B) as a Function of Internuclear Separation.

Table 14. Molecular Constants for the $a^3\Sigma_u^+$, $b^3\Pi_g$, and $F^1\Pi_u$ Electronic States[a]

Property	$a^3\Sigma_u^+$	$b^3\Pi_g$	$F^1\Pi_u$
r_e Theo.	1.0493	1.0681	1.0869
Exp.	1.0457	1.0635	1.0849
T_e[b]	143768.	148962.	165665.
	144048.	148835.	165971.
		(5194.)	(21897.)
		(4787.)	(21923.)
ω_e[c]	1816.	1766.	1673.
	1809.	1769.	1671.
D_e[d]	15636.	19942.	5293.
	15806.		

[a] All distances in agnstroms and energies in cm-1. Experimental data from Huber and Herzberg (1979).
[b] The first set of values are T_e with respect to the $X^1\Sigma_g^+$ at R=40 au, and the parenthetical values are T_e's with respect to the E_e of $a^3\Sigma_u^+$.
[c] Theoretical ω_e's from $\Delta G(2\text{-}1) - \Delta G(1\text{-}0) = -2\omega_e x_e$ and $\omega_e = G(1\text{-}0) + 2\omega_e x_e$ (Herzberg 1950).
[d] Determined from the energy difference between r_e and R=40 au.

Table 15. Barrier Heights and Barrier Positions for the $a^3\Sigma_u^+$ and $F^1\Pi_u$ States

	This Study		Previous Theory		Experiment	
State	Height[a]	Position[b]	Height	Position	Height	Postion
$a^3\Sigma_u^+$	1.56	2.70	2.7	2.9[c]	1.82[e]	
			1.85	2.68[d]	1.55	2.77[f]
			1.507	2.712[j]	1.43±.05	2.72±.04[g]
$F^1\Pi_u$	10.9	1.79	13.5	1.73[h]		
			12.5[i]	1.78[i]		

[a] Energies in kcal/mol.
[b] Distances in Angstroms.
[c] Peach (1978).
[d] MCSCF calculations (Sunil et al. 1983).
[e] Lundlum, Larson, and Caffrey (1967).
[f] Brutschy and Haberland (1979).
[g] Jordan, Siddiqui, and Siska (1986).
[h] Valence-bond calculations (Gupta and Matsen 1969).
[i] Browne (1965).
[j] Large-scale MCSCF plus second-order CI (Konowalow and Lengsfield 1987).

One can immediately see that much of the contribution to the total perturbation is excluded from the Ψ's if the only interaction allowed with $a^3\Sigma_u^+$ and $X^1\Sigma_g^+$ is with the lowest energy $^1\Pi_u$ or $^3\Pi_g$ state, respectively. This type of analysis highlights the importance of including higher lying excited states (a benefit of this method) and points to the possible danger of premature truncation which is an intrinsic problem when one tries to represent Ψ^1 as a sum of interactions over discreet eigenstates as represented by Equation 1.

The total electric transition dipole moment, as well as it's two components (see Equation 5) are plotted in Figure 3. It can be seen that the singlet component dominates over most of the $a^3\Sigma_u^+$ bound potential, with the triplet component having comparable magnitude only at small internuclear separations. The two moments have opposite signs for values less than 2.0 bohr, and then remain the same sign up through r=3.5, after which they are again opposites. The difference in signs at small internuclear separation causes a cancellation in forming the total transition moment, generating a near zero moment at r=1.50 bohr. From r=1.85 onward the total transition dipole is essentially determined by the singlet component which has a maximum value of 6.0×10^{-6} au at r=3.8.

If we wish to give an explanation for the shape of μ_1, we need to look primarily at the singlet states and, in particular, the $^1\Pi_u$ states. The hump in the $F^1\Pi_u$ occurs due to an avoided crossing of this state with higher lying $^1\Pi_u$ states. One theoretical study (Gupta and Matsen 1969) dissociates to the ls+1s3d limit. The location of the $F^1\Pi_u$ hump in the PEC at r=1.85 Å (in the current study) lies reasonably close to the maximum at r=2.1 Å in the singlet component of the transition moment (see Figure 3). The $a^3\Sigma_u^+$-$^1\Pi_u$ S-O interaction also shows a maximum at r=2.1 Å (see Figure 1, Curve A). It would appear, therefore, that the $\langle a^3\Sigma_u^+ | H^{so} | {}^1\Pi_u \rangle$ S-O perturbation and the singlet contribution to μ_1 (and hence the total μ_1) depend not only upon interactions with the $F^1\Pi_u$ but also with higher lying $^1\Pi_u$ states.

The results of the vibrational analysis are given in Table 16, where one finds the predicted lifetime of the v=0 level in $a^3\Sigma_u^+$ to be 18 sec, which is consistent with the more current experimental prediction of 10 sec for a lower bound (Mehrotra, Mann, and Dahm 1979). The lifetimes are seen to monotonically decrease with increasing vibrational quantum number, at least up to v=9. At v=5 the lifetime falls below the predicted lower bound of 10 sec, suggesting that the majority of excited He_2 neutrals observed by Mehrotra, Mann, and Dahm (1979) in their experiment reside in the v=0 to v=4 or 5 levels.

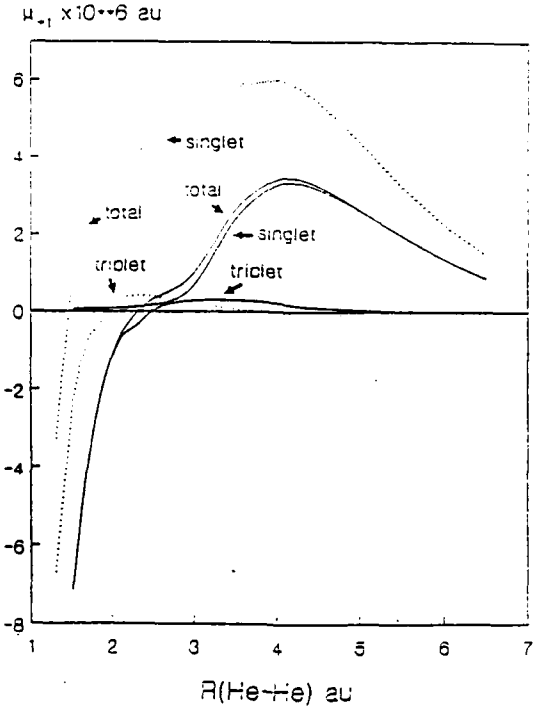

Figure 3. (...); Singlet and Triplet Components of Electric Transition Dipole Moment for $X^1\Sigma_g^+ \leftarrow a^3\Sigma_u^+$ With Perturbations From the Full $^1\Pi_u$ and $^3\Pi_g$ State Manifold. (____); Singlet and Triplet Components With Perturbation From Only the $F^1\Pi_u$ or $b^3\Pi_g$ State

Table 16. Results from Vibrational Analyses of the $a^3\Sigma_u^+$, $b^3\Pi_g$, and $F^1\Pi_u$ States with Energies in cm^{-1} and Lifetimes, τ, in Seconds.

	v	$a^3\Sigma_u^+$ Energy	τ	$b^3\Pi_g$ Energy	$F^1\Pi_u$ Energy
	0	899	00000?	873	826
00143?	1	2635	15	2570	2420
	2	4290	13	4199	3926
	3	5867	12	5757	5270
	4	7373	11	7242	
	5	8785	9.6	8658	
	6	10097	8.5	10000	
	7	11306	7.5	11270	
	8	12433	6.7	12459	
	9	13452	6.0	13569	

6. THE INTERACTION OF HYDROGEN CHLORIDE WITH RARE GAS ATOMS

Recently, Fajardo and Apkarian (1986, 1988a, 1988b) published experimental results documenting long term energy storage (one to two days) in solid Xe. The phenomenon depends upon the formation (via laser excitation) and separation of a stable, negatively charged exciplex such as Cl^-Xe_2 and a self-trapped positive hole (STH) localized on a Xe_n^+ (n=2 or 3) molecule. The first step in the formation of these separated polarons is a cooperative charge transfer excitation involving molecular Cl_2 or HCl and the Xe atoms in the solid to form:

$$Xe + HCl + 2h\nu \rightarrow Xe^+(HCl)^-$$

which quickly reacts with another Xe atom to form the more stable triatomic exciplex $Xe_2^+Cl^-$. This exciplex decays primarily from the $4^2\Gamma$ state through a radiative process with a natural lifetime of 225 nsec[2]. The stability of the STH is related to the stabilization energy associated with crystal relaxation effects. A more recent publication by Schwentner, Farjardo, and Apkarian (1989) gives another description of the charge transfer (CT) excitation as a Rydberg progression of hole states. Last and George (1988) have published some theoretical work on Xe_nHCl clusters, predicting transition energies and various stable and various quasi-stable structures for the ground and several excited electronic states. They developed and used a semi-empirical method called diatomics-in-ionic-systems, or DIIS, which enabled them to include many Xe atoms.

As an extension to our earlier studies of rare gas (RG) atomic and molecular interactions (Chabalowski et al. 1989; Perry and Yarkony 1988), we begin this preliminary theoretical treatment of the RG halide interactions by studying the interactions of HCl with Xe atoms. Quantum chemical calculations are performed on the ground and excited states of HCl (not reported here), XeCl, and HClXe, including state-averaged CASSCF (Lengsfield 1982) and CI calculations.

6.1 Details of Calculations. All calculations were carried out in the C_{2v} point group. The atomic basis sets used are a combination of Gaussian-type orbitals (GTO) and the effective core potentials (ECP) of Wadt and Hay (1985). The ability of our codes to handle ECPs allows for the treatment of systems including such heavy atoms as Xe. The gaussian basis consists of a non-contracted set of four s-type primitives and one p-type polarization function, (α_p=1.0), on hydrogen, giving [4s/1p]. The chlorine basis contains three non-contracted s- and p-type valence AOs with exponents optimized for their use with the ECPs (Wadt and Hay 1985). This is augmented by a negative ion function (α_p=0.049) and a polarization function (α_d=0.50), for a total basis set of [3s,3p/1p,1d]. Likewise, the

Xe basis associated with the ECPs consists of three s- and p-type primitives which are contracted to double-zeta (Wadt and Hay 1985) augmented by a single polarization function, (α_d=0.25), giving [2s,2p/1d].

The orbitals used as expansion vectors in the CI are obtained by state-averaging in a CASSCF, thereby generating orbitals suitable to both the ground and excited states. These preliminary wavefunctions are generated from the ALCHEMY code (Lui and Yoshimine 1981) by doing all single and double electronic excitations from a set of reference CSFs. Due to the exploratory nature of these calculations, rather small CI expansions were used. PECs and electronic transition dipole moments are then calculated and used to explicitly include the vibrational motion of the nuclei, enabling us to predict transition probabilities and radiative lifetimes. One potential weakness in these calculations is the neglect of S-O interactions. But earlier theorical work done by Hay and Dunning (1978) on XeCl showed that much useful qualitative and semi-quantitative information can be obtained without inclusion of S-O effects. Our codes already include these effects for the lighter atoms where use of the Briet-Pauli Hamiltonian is appropriate, and plans have already been laid for including in our codes S-O effects in heavy atoms.

6.2 Xe-Cl Interactions. To help determine the suitability of the ECPs for studying the HCl-Xe interactions, we have first calculated the PECs and transition probabilities for the Xe-Cl system which has already been studied both theoretically (Hay and Dunning 1978) and experimentally (Inoue, Ku, and Setser 1984). We calculate the $1,2^2\Sigma^+$ and the $1,2^2\Pi$ states and the strong $2^2\Pi$->$1^2\Pi$ and $2^2\Sigma^+$->$1^2\Sigma^+$ transitions, as well as the weak $2^2\Pi$->$1^2\Sigma^+$ and $2^2\Sigma^+$->$1^2\Pi$ transitions, reporting lifetimes for emissions from the v'=0 levels. This is believed to be the first time that the lifetimes have been calculated theoretically for the weak transitions.

The PECs can be seen in Figure 1, and some molecular constants are reported in Table 1, along with values from earlier theoretical work by Hay and Dunning (1978). Hay and Dunning had calculated the electronic states both with and without S-O effects, and both values are reported in Figure 1. Our equilibrium bond lengths and ω_e's are in reasonably good agreement with Hay and Dunning's values. It is worth pointing out that the R_e's and ω_e's of Hay and Dunning are almost unaffected by the inclusion of S-O. Figure 2 gives the electric transition dipole moments for the strong transitions as a function of R(Xe-Cl). Near the R_e (6.4 bohr) values for the $2^2\Sigma^+$ excited state, the moment for the Σ-Σ transition is approximately 4.5 times greater than the Π-Π moment. The

transition moments and PECs from this work are nearly identical to those calculated by Hay and Dunning when S-O is ignored. Table 17 also includes the results of our vibrational analysis for the radiative lifetimes. Again, our predicted lifetimes for the strong transitions are very similar to Hay and Dunning's without S-O effects. In this case, the S-O makes a difference by nearly doubling the natural lifetimes for both the $^2\Sigma^+$ and $^2\Pi$ states. Hay and Dunning's lifetimes with S-O are amazingly close to the experimental approximations to the correct state descriptions due to mixing of different Λ components of Ω through the S-O operator.

Figure 3 shows the transition moments for the weak transitions and the resulting lifetimes are listed in Table 1. These excited states are predicted to have lifetimes on the order of 26 μsec and 104 μsec for the $2^2\Pi$-$1^2\Sigma$ and $2^2\Sigma$-$1^2\Pi$ transitions, respectively. These are several orders of magnitude greater than the lifetimes for the strong transitions.

6.3 Xe--HCl Interactions. HCl-XE is treated as a linear system with the Xe opposite the hydrogen atom. Calculations were performed at nuclear separations of R=(6.425, 7.0, 8.0, 10.0, 15.0, 20.0) while holding R(HCl) at R_e (HCl)=2.409 bohr. The lowest two states of $^1A_1$ symmetry and the lowest three states of $^1B_1$ (Π_x) symmetry were calculated. The states of interest are the $1^1A_1(X^1\Sigma^+)$, $1^1B_1(A^1\Pi)$, and 2^1B_1, which turns out to be a CT state with an electron going from the Xe(p_x) doubly occupied MO to a H-Cl (σ^*-antibonding) MO. This 2^1B_1 (CT) state could then be responsible for the CT and subsequent breaking of the H-Cl bond. The 2^1B_1 (CT) lies above the HCl $A^1\Pi$ valence state. The $A^1\Pi$ state is essentially localized on the HCl, and in the isolated HCl the $A^1\Pi$ state is the lowest excited singlet and everywhere repulsive, dissociating to the same asymptote as the ground state (Stevens and Krauss 1982; Last and George 1988). It will be interesting to see if the 2^1B_1 (CT) state (or its equivalent) becomes the lowest excited state when more Xe atoms are added. The third state of B_1 symmetry in Figure 4 is a mixture of many CSFs but predominantly described by exciting an electron from the HCl sigma bond to the negative ion Cl(p_x) MO. This is most likely a state trying to be Rydberg in nature but due to the lack of true Rydberg AOs in the basis it is poorly represented.

Finally, we can look at the electric dipole moments for the transitions $A^1\Pi$ -- $X^1\Sigma^+$ (T1) and 2^1B_1 (CT) -- $X^1\Sigma^+$ (T2) shown in Figure 5. In isolated HCl, this study calculates T1 to be 0.32 D at R=2.4 bohr (near R_e[HCl]). The values for the transition moment of T1 is seen to approach this value as R(HCl-XE) $\rightarrow$ 20 bohr. Its asymptotic value falls short of the .32 D found in HCl, most likely due to

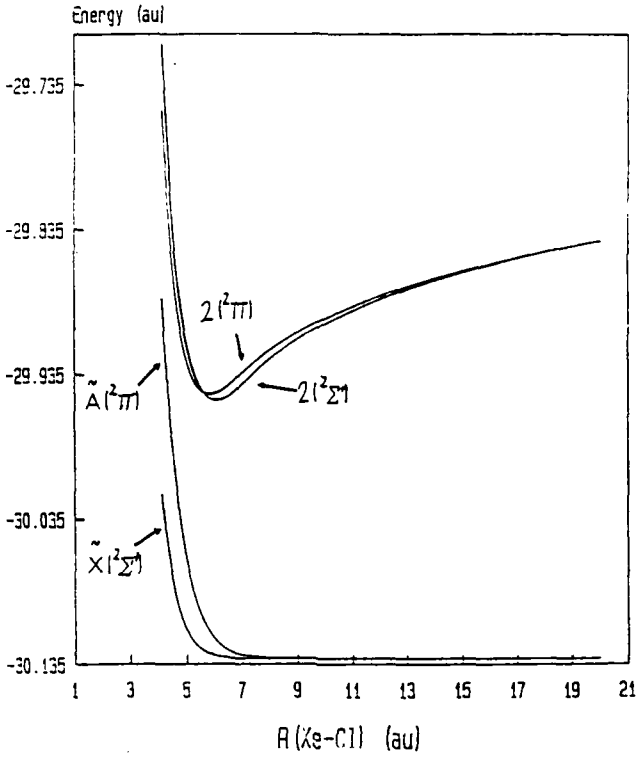

Figure 4. Potential Energy Curves for 1, $2^1\Sigma^1$ and 1, $2^2\Pi$ Without S-O in XeCl.

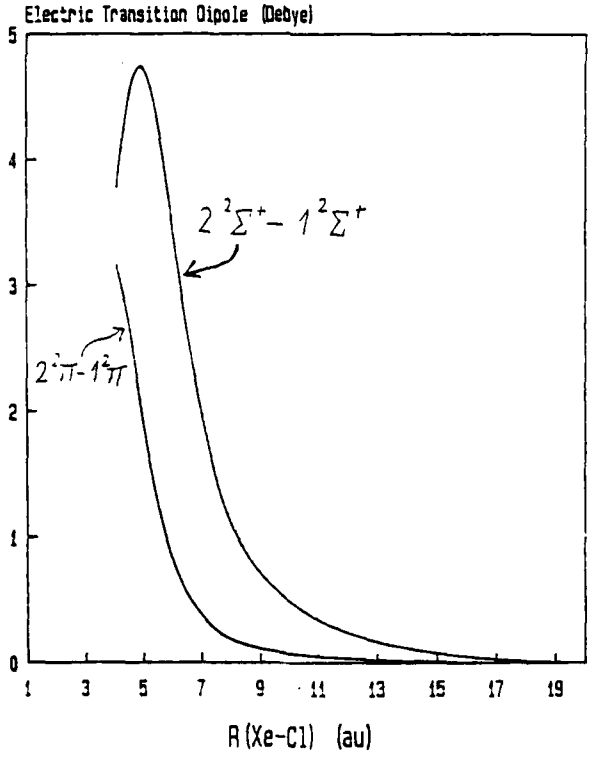

Figure 5. Electric Transition Dipole Moments for the Sigma-Sigma and Pi-Pi Spin-Allowed Doublet Transition in XeCl.

Table 17. Molecular Constants for XeCL

	R_e(Å)			ω_e(cm^{-1})		
	This Study	H & D[a] (No S-O)	H & D (With S-O)	This Study	H & D (No S-O)	H & D (With S-O)
$2^2\Sigma^+$	3.20	3.25	3.22	198.	190.	188.
$2^2\Pi$	3.08	3.14	3.14	196.	188.	188.

Radiative Lifetimes (nsec)				
	This Study	H & D[a] (No S-O)	H & D (With S-O)	Experimental[b]
$2^2\Sigma^+ - 1^2\Sigma^+$	6.0	5.6	11.	11.1
$2^2\Pi - 1^2\Pi$	74.	64.	120.	131.
$2^2\Pi - 1^2\Sigma^+$	26. μsec			
$2^2\Sigma^+ - 1^2\Pi$	104. μsec			

[a] DZP+First-Order POL-CI (Hay and Dunning 1978).
[b] Inoue, Ku, and Setser (1984).

a slight difference in the details involved in generating the CI expansion vectors from the state-averaged CASSCF. We expect that for calculations using better AO basis sets and larger CI expansions this discrepency should disappear. The reader should note the increase in the moment for T2 as R(HCl-Xe) approaches what is reported to be near the equilibrium distance of R(CL-Xe)=6.4 bohr in the exciplex $Xe_2^+Cl^{-1}$. At this point, the moment for T2 is about equal to the transition moment for T1. It is interesting to speculate what the size of the transition moment will be for the CT transition when more Xe atoms are included. One also notices that the moment for the CI transition is largest at about R=8.0 bohr. This is consistent with the notion that the neutral Cl and Xe atoms (at the onset of excitation) will most likely be at a R(Xe-Cl) distance which is larger than $R(Xe^+Cl^-)$=6.4 bohr.

Clearly, much insight into the XeCl interactions can be achieved through the combination of effective core potentials and wavefunctions obtained from state-averaged MCSCF and CI. The results compare favorably with earlier *ab initio* work, although the difference in radiative lifetimes predicted

by Hay and Dunning both with and without spin-orbit effects highlight the need for inclusion of such effects.

The results for HCl-Xe identified a CT state as the second highest excited state of $^1\Pi$ symmetry. This state drops in energy as the R_e for the exciplex is approached. This CT state represents promotion of an electron into a HCl σ^*-antibonding orbital. This process may account for the formation of the Cl atom upon excitation in the solid. The predicted changes in transitions moments suggest an enhanced probability for populating this CT state at internuclear distances similar to those in the Xe solid.

More general calculations on HClXe are planned. These employ a larger, more flexible AO basis set including Rydberg functions, and larger CI wavefunction expansions with additional electronic states in both the $^1A_1$ and $^1B_1$ symmetries included. We have also begun calculations that included a second Xe atom in the model. The low lying electronic states are being calculated for $HClXe_2$ and the transition probabilities amongst these states will be predicted. Our initial study addresses linear geometries, but other structures will be explored including the conformation in which Xe-Cl-Xe forms an isosceles triangle. That structure is predicted to a global energy minimum on the potential energy surface by Stevens and Krauss (1982).

7. METHOD DEVELOPMENT

An integral part of this research was the extension of the theoretical capabilities of the BROOKLYN suite of quantum chemistry codes for treating spin-forbidden and electronically nonadiabatic processes using the computational facilities available in our laboratory. In particular, we have added the capability to treat the dipolar spin-spin interaction and the extended capabilities for treating first and second derivative nonadiabatic coupling matrix elements which incorporate the computational economies and conceptual simplifications afforded by the explicit use of the body fixed frame symmetries.

8. APPLICATIONS

In our applications we have considered the stability of proposed high-energy density material with respect to radiative and radiationless decay. These studies provide a clear demonstration of the power

of theoretical methods to (quickly) assess the utility of a proposed energy storage system by determining the topology of the relevant potential energy surfaces (PESs) and the nonadiabatic interactions which couple them. We have used our methods to characterize the interaction between a heltium atom and a hydrogen molecule excited to the $B^1\Sigma_u^+$ electronic state.

The $H_2(B^1\Sigma_u^+)$ state contains more that 11 eV of energy relative to the $H_2(X^1\Sigma_g^+)$ ground state (Huber and Herzberg 1979). It has been suggested that the CT structure $(HeH)^+$-H^- which consists of two stable moieties, HeH^+ and H^-, might exist as a stable species on either the $2^1A'$ PES as a maximum ionicity excited state (MIES) (Farantos, Theodorakopoulos, and Nicolaides 1983) structure or on the ground $1^1A'$ PES and thereby provide a chemical means of storing the electronic energy in the $B^1\Sigma_u^+$ state of H_2.

To consider these possibilities, the $1,2^1A'$ states of He-H_2 system were characterized using *ab initio* MCSCF/second order CI wavefunctions (Lengsfield 1982). These surfaces correlate with the $He(^1S)$ + $H_2(X^1\Sigma_g^+, B^1\Sigma_u^+)$ system states. This work provided the first extended treatment of the nonadiabatic interactions between the $1,2^1A'$ states reporting first derivative nonadiabatic couplings at over 100 nuclear configurations. Two extrema on the $2^1A'$ PES were determined at the CI level, a global minimum and a saddle point. In each case the character of the extremum was determined from the eigenvalues of the second derivative matrix. While this work built on previously reported theoretical treatments of these PESs (Farantos, Murrell, and Carter 1984), both qualitative and quantitative differences with previous work were found. The predicted, entrance channel, saddle point on the $2^1A'$ PES has a barrier of 1.5 Kcal/mol, significantly lower than the previous estimates (Grimes, Lester, and Dupuis 1986), but in good accord with recent experimental results from C. B. Moore's group presented at the HEDM Contractor's Conference (Pibel, Kung, and Moore 1989). The global minimum on the $2^1A'$ PES corresponds to a CT structure, $(HeH)^+$-H^- and is stable by 38.99 Kcal/mol relative to the $He(^1S)$ + $H_2(B^1\Sigma_u^+)$ asymptote. The structure and the energy of this extremum are in qualitative accord with the previous *ab initio* results of Farantos, Theodorakopoulos, and Nicolaides (1983).

The most significant finding in this work was the demonstration of the existence of a seam for which the $1^1A'$ and $2^1A'$ PESs are nearly degenerate, $\Delta E \equiv E(2^1A') - E(1^1A') < 0.001$-$0.5$ Kcal/mol. This extended region of large, nonadiabatic effects occurs for general C_s, rather than C_{2v} or $C_{\infty v}$ geometries, and includes the region of the minimum on the $2^1A'$ PES noted above. This feature of the

$1,2^1A'$ PESs should significantly influence the quenching of $H_2(B^1\Sigma_u^+)$ by He and alter expectations of the lifetime of the state corresponding to the global minimum on the $2^1A'$ PES (Farantos and Tennyson 1985). It is anticipated that the lower entrance channel barrier noted above, and the near degeneracy seam reported here, will serve to increase the calculated cross section (Farantos 1985) which is appreciably lower than the measured value (Akins, Fink, and Moore 1970; Fink, Adkins, and Moore 1972). The large, nonadiabatic coupling between the $1,2^1A'$ wavefunctions in the vicinity of the global minimum on the $2^1A'$ PES will serve to decrease the predicted lifetime of this "state." To facilitate dynamical studies of these questions, first derivative nonadiabatic coupling matrix elements were determined in the vicinity of the "seam."

The possible stability of the CT structure $(HeH)^+$-H^- on the $1^1A'$ PES was considered using a surface walking technique. In the vicinity of the above noted seam exchange of the CT structure between the $1,2^1A'$ states is observed. Surface walks on the $1^1A'$ PES which follow the energy gradient from nuclear configurations corresponding to the CT structure, $(HeH)^+$-H^-, were performed. In no case was a stable triatomic structure corresponding to a CT configuration found.

9. REFERENCES

Adams, G. F., M. M. Gallo, and M. Page. "Extended Basis Set Calculations of Atomization Energies: Comparison of Direct and Isogyric Methods." Chem. Phys. Letters, vol. 162, p. 497, 1989.

Adams, G. F., and M. Page. "Structures and Energies for Small Borane Compounds. One and Two Boron Compounds." BRL Technical Report, to be published.

Amos, R. D., and J. E. Rice. The Cambridge Analytic Derivatives Package. Version 4, 1988.

Akins, D. L., E. H. Fink, and C. B. Moore. "Rotation Translation Energy Transfer Between Individual Quantum States of HD ($B^1\Sigma_u^+$)." J. Chem. Phys., vol. 52, p. 1604, 1970.

Browne, J. C. "Quantum Mechanical Potential Energy Curves for the (1)Πu and (3)Πu States of He2 and the (1)Πg and (3)Πg States of H2." Phys. Rev. 1A, vol. 138, p. 9, 1965.

Brutschy, B., and H. Haberland. "Lang-range Helium Excimer Potentials (A,C[1]Σu,g and a, c (3)Σu,g) From High-resolution Differential Cross Sections for He(2[1]S, s[3]S)+He." Phys. Rev., vol. 19, p. 2232, 1979.

Calvani, P., B. Maraviglia, and C. Messana. "Propagation of Neutral Excitations In He II At T>O.9 K." Phys. Letters, vol. 39A, p. 123, 1972; and references therein.

Carter, E., and W. A. Goddard, III. "Correlation Consistent Configuration Interaction: Accurate Bond Dissociation Energies From Simple Wavefunctions." J. Chem. Phys., vol. 88, p. 3132, 1988.

Chabalowski, C. F., J. O. Jensen, D. R. Yarkony, and B. H. Lengsfield III. "Theoretical Study of the Radiative Lifetime for the Spin-forbidden Transition a(3)Σu→X(1)Σg in He2." J. Chem. Phys., vol. 90, p. 2504, 1989.

Fajardo, M. E., and V. A. Apkarian. "Cooperative Photoabsortion Induced Charge Transfer Reaction Dynamics in Rare Gas Solids. I. Photodynamics of Localized Xenon Chloride Exciplexes." J. Chem. Phys., vol. 85, p. 5660, 1986.

Fajardo, M. E., and V. A. Apkarian. "Charge Transfer Photodynamics in Halogen Doped Xenon Matrices. II. Photo-induced Harpooning and the Delocalized Charge Transfer States of Solid Xenon Halides (F,Cl,Br,I)." J. Chem. Phys., vol. 89, p. 4102, 1988a.

Fajardo, M. E., and V. A. Apkarian. "Energy Storage and Thermoluminescence in Halogen Doped Solid Xenon. III. Photodynamics of Charge Separation, Self-trapping, and Ion-hole Recombination." J. Chem. Phys., vol. 89, p. 4124, 1988b.

Farantos, S. C. "A Classical Study of Collisions of He with HD($B^1\Sigma_u^+$)." Mol. Phys., vol. 54, p. 835, 1985.

Farantos, S. C., J. N. Murrell, and S. Carter. "Analytical *ab initio* Potential Energy Surfaces for the Ground and First Singlet Excited States of HeH_2." Chem. Phys. Letters, vol. 108, p. 367, 1984.

Farantos, S. C., G. Theodorakopoulos, and C. A. Nicolaides. "A Non-van der Waals Minimum of the He + H_2 Excited Surface." Chem. Phys. Letters, vol. 100, p. 263, 1983.

Farantos, S. C., and J. Tennyson. "Rovibrational Spectrum of the Excited Potential Energy Surface of He + H_2 ($B^1\Sigma_u^+$)." J. Chem. Phys., vol. 82, p. 2163, 1985.

Fink, E. H., D. L. Atkins, and C. B. Moore. "Energy Transfer in Monochromatically-Excited Hydrogen ($B^1\Sigma_u^+$). I. Excitation Processes, Electronic Quenching, and Vibrational Energy Transfer." J. Chem. Phys., vol. 56, p. 900, 1972.

Grimes, R. M., W. H. Lester, and M. Dupuis. "Coupled Channel Study Rotational Excitation of an Electronically Excited Diatomic Molecule by Atom Impact: He(s) + H_2." J. Chem. Phys., vol. 84, p. 5437, 1986.

Gupta, B. K., and F. A. Matsen. "Quantum-Mechanical Study of the F(1)Πu and f(3)Πu States of He2." J. Chem. Phys., vol. 50, p. 3797, 1969.

Handy, N. C. "The Value of High Accuracy Calculations in Quantum Chemistry." Faraday Symp. Chem. Soc., vol. 10, p. 17, 1986.

Havriliak, S. J., and D. R. Yarkony. "On the Use of the Breit-Pauli Approximation for Evaluating Line Strengths for Spin-Forbidden Transitions: Application to NF." J. Chem. Phys., vol. 83, p. 1168, 1985; and references therein.

Hay, P. J., and T. Dunning. "The Covalent and Ionic States of the Xenon Halides." J. Chem. Phys., vol. 69, p. 2209, 1978.

Herzberg, G. Spectra of Diatomic Molecules. New York: Van Nostrand-Rheinhold, 1950.

Huber, K. P., and G. Herzberg. Molecular Spectra and Molecular Structure. New York: Van Nostrand-Rheinhold, 1979.

Inoue, G., J. K. Ku, and D. W. Setser. "Photoassociative Laser-induced Fluorescence of XeCl* and Kinetics of XeCl(B) and XeCl(C) in Xe." J. Chem. Phys., vol. 80, p. 6006, 1984.

Jordan, R. M., H. R. Siddiqui, and P. E. Siska. "Potential Energy Curves for the a(3)Σu and c(3)Σg States of He2 Consistent With Differential Scattering, *Ab Initio* Theory, and Low-temperature Exchange Rates." J. Chem. Phys., vol. 84, p. 6719, 1986.

Konowalow, D. D., and B. H. Lengsfield III. "The Electronic and Vibrational Energies of Two Double-welled (3)Σu States of He2." J. Chem. Phys., vol. 87, p. 4000, 1987.

Krishnan, R., J. S. Binkley, R. Seeger, and J. A. Pople. "Self-consistent Molecular Orbital Methods XX. A Basis Set for Correlated Wavefunctions." J. Chem Phys., vol. 72, p. 650, 1980.

Lammertsma, K. Private communication, February 1990.

Last, I., and T. F. George. "Electronic States of the XennHCL Systems in Gas and Condensed Phases." J. Chem. Phys., vol. 89, p. 3071, 1988.

Lengsfield III, B. H. "General Second-order MCSCF Theory for Large CI Expansions." J. Chem. Phys., vol. 77, p. 4073, 1982.

Lengsfield III, B. H. Private communication, February 1990.

Liu, B., and M. Yoshimine. "The ALCHEMY Configuration Interaction Method. I. The Symbolic Matrix Method of Determining Elements of Matrix Operators." J. Chem. Phys., vol. 74, p. 612, 1981.

Lundlum, K. H., L. P. Larson, and J. M. Caffrey. "Activation Energy for the Three-body Reaction of Helium Triplet Atom with Normal Helium." J. Chem. Phys., vol. 46, p. 127, 1967.

Mehrotra, R., E. K. Mann, and A. J. Dahm. "A Study of the Neutral Excitation Current In Liquid He Above 1 K." J. Low Temp. Phys., vol. 36, p. 47, 1979.

Montgomery, J., and H. H. Michels. Private communication, May 1987.

Nicolaides, C. A., G. Theodorapoulis, and I. D. Petsalakis. "Theory of Chemical Reactions of Vibrationally Excited $H_2(B^1\Sigma_u^+)$. I. Prediction of a Strongly Bound Excited State of H_4. J. Chem. Phys., vol. 80, p. 1705, 1984.

Page, M. "Multireference CI Study of the Reaction $H_2 + BO \rightarrow H + HBO$." J. Phys. Chem., vol. 93, p. 3639, 1989.

Peach, G. "Low-energy Scattering of Excited Helium Atoms by Rare Gases I. The Model Potentials." J. Phys., vol. B11, p. 2107, 1978.

Perry, J. K., and D. R. Yarkony. "On the Electronic Structure of the $He+H_2$ System: Characterization of, and Nonadiabatic Interactions Between, the 1(1)A′ and 2(1)A′ Potential Energy Surfaces." J. Chem. Phys., vol. 89, p. 4945, 1988.

Pibel, C. H., A. H. Kung, and C. B. Moore. "Abstracts of HEDM Contractors Conference," New Orleans, LA, 1989.

Pople, J. A., M. J. Frisch, B. T. Luke, and J. S. Binkley. "A Moller-Plesset Study of the Energies of AH_n Molecules (A= Li to F)." Int. J. Quantum Chem., S17, p. 307, 1983.

Schwenter, N., M. E. Fajardo, and V. A. Apkarian. "Rydberg Series of Charge Transfer Excitations in Halogen-doped Rare Gas Crystals." Chem. Phys. Letters, vol. 154, p. 237, 1989.

Stevens, W. J., and M. Krauss. "Absorption in the Triatomic Excimer, Xe2Cl." Appl. Phys. Letters, vol. 41, p. 301, 1982.

Sunil, K. K., J. Lin, H. Siddiqui, P. E. Siska, K. D. Jordan, and R. Shepard. "Theoretical Investigation of the a, A, c, and C Potential Energy Curves of He2 and of He*(2[1]S,2[3]S)+He Scattering." J. Chem. Phys., vol. 78, p. 6190, 1983.

Surko, C. M., and F. Reif. "Investigation of a New Kind of Energetic Neutral Excitation In Superfluid Helium." Phys. Rev., vol. 175, p. 229, 1968.

Surko, C. M., and F. Reif. "Evidence For a New Kind of Energetic Neutral Excitation In Superfluid Helium." Phys. Rev. Letters, vol. 20, p. 582, 1968.

Wadt, W. R., and P. J. Hay. "*Ab Initio* Effective Core Potentials for Molecular Calculations. Potentials for Main Group Elements Na to Bi." J. Chem. Phys., vol. 82, p. 284, 1985.

Yarkony, D. R. "On the Radiactive Lifetimes of the b(1)Σ(+) and a(1)Δ States In NCl." J. Chem. Phys., vol. 86, p. 1642, 1987; and references therein.

Yarkony, D. R. "Spin Forbidden Radiactive Decay Involving Quasi-degenerate States. Application to the $B^1\Sigma^+ \rightarrow a^3\Pi$ Transition in MgO." J. Chem. Phys., vol. 89, p. 7324, 1988.

Yarkony, D. R. "On the Quenching of Helium 2^3S: Potential Energy Curves for, and Nonadiabatic, Relativistic, and Radiactive Couplings Between the $a^3\Sigma_u^+$, $A^1\Sigma_u^+$, $b^3\Pi_g$, $B^1\Pi_g$, $c^3\Sigma_g^+$ and $C^1\Sigma_g^+$ States of He_2." J. Chem. Phys., vol. 90, p. 7164, 1989.

BIBLIOGRAPHY

1. Adams, G. F., M. M. Gallo, and M. Page. "Extended Basis Set Calculations of Atomization Energies: Comparison of Isogyric and Direct Results." Chem. Phys. Letters, vol. 162, p. 497, 1989.

2. Chabalowski, C. F., J. O. Jensen, D. R. Yarkony, and B. H. Lengsfield III. "Theoretical Study of the Radiative Lifetime for the Spin-Forbidden Transition $a^3\Sigma_u^+ \rightarrow X^1\Sigma_g^+$ in He_2 Using *Ab Ibitio* State Averaged MCSCF Plus CI Methods." J. Chem. Phys., vol. 90, p. 2504, 1989.

3. Jensen, J. O., G. F. Adams, and C. F. Chabalowski. "*Ab Initio* Study of the Electronic Magnetic Circular Dichroism Spectrum in Acetylene: The $B \leftarrow X$ and $1'B_2 \leftarrow X$ Transitions." J. Chem. Phys., accepted for publication.

4. Jensen, J. O., G. F. Adams, and C. F. Chabalowski. "*Ab Initio* Study of the Dipole Transition Moment for the $C \leftarrow X$ Electronic Transition in Acetylene: Theoretical Predictions of the Absorption and Magnetic Circular Dichroism Intensities." Chem. Phys. Letters, in press.

5. Jensen, J. E., and D. R. Yarkony. "On the Characterization of the Dipolar Spin-Spin Interaction in Molecular Systems: A Symbolic Matrix Element Q Approach." Chem. Phys. Letters, vol. 141, p. 391, 1987.

6. Konowalow, D. D., and B. H. Lengsfield III. "The Electronic and Vibrational Energies of Two Double-welled $3\Sigma_u^+$ States of He_2." J. Chem. Phys., vol. 87, p. 4000, 1987.

7. Lengsfield III, B. H., and D. R. Yarkony. "On the Evaluation of Nonadiabative Coupling Matrix Elements for MCSCF/CI Wavefunctions Using Analytic Derivative Methods. III. Second Derivative Terms." J. Chem. Phys., vol. 84, p. 348, 1986.

8. Saxe, P., and D. R. Yarkony. "On the Evaluation of Nonadiabative Coupling Matrix Elements for MCSCF/CI Wavefunctions. IV. Second Derivative Terms Using Analytic Gradient Methods." J. Chem. Phys., vol. 86, p. 321, 1987.

9. Yarkony, D. R. "On the Use of the Breit-Pauli Approximation for Evaluating Linestrengths for Spin-Forbidden Transitions II: The Symbolic Matrix Element Method." J. Chem. Phys., vol. 84, p. 2075, 1986.

INTENTIONALLY LEFT BLANK.